A THERMODYNAMIC ANALYSIS OF THE Al-Zn SYSTEM AND PHASE DIAGRAM CALCULATION

Shuang-Lin Chen and Y. A. Chang

Department of Materials Science and Engineering
University of Wisconsin-Madison
1509 University Avenue
Madison, Wisconsin 53706
U. S. A.

ABSTRACT Using the Redlich-Kister expression to represent the Gibbs energies of the liquid, fcc and hcp phases in the Al-Zn binary system, the model parameter values were obtained by optimization using thermodynamic and phase equilibrium data available in the literature. Not only are the model-calculated values for the thermodynamic properties in agreement with the available experimental data, but also the calculated phase diagram is in agreement with the phase boundary data. The thermodynamic description obtained in the present study is an improvement over the previous descriptions reported in the literature.

1. Introduction

As part of of a study to develop a thermodynamic description for multi-component aluminum alloys of technological importance, several binary systems have been evaluated thermodynamically by us. These binary systems are Al-Li [89Che], Al-Mg [92Zuo], Cu-Li [91Che] and Cu-Mg [92Zuo]. In the present study, we wish to report the results of our study for the Al-Zn binary system. Complete thermodynamic descriptions of the binaries are needed prior to developing thermodynamic descriptions of ternary and high-order aluminum systems. Coupling thermodynamic descriptions with solidification, diffusion, heat transfer, etc., ultimately allows us to define processing conditions quantitatively to make materials with desired properties.

The phase relationships for Al-Zn are relatively simple. There are only three solution phases, i.e., the liquid, fcc and hcp phases. There exist three invariant equilibria in the Al-Zn system. They are the eutectic equilibrium, L=fcc+hcp, at 654K, the critical point for phase separation of the fcc phase, $fcc=fcc_1+fcc_2$, at 624.5K, and the monotectoid equilibrium, i.e., $fcc_2=fcc_1+hcp$, at 550K. The thermodynamic and phase equilibrium data were critically assessed by Hultgren *et al.* [73Hul2] and most recently by Murray [83Mur]. As part of her study, Murray attempted to develop a thermodynamic description for this binary system. Two sets of parameters for the three phases were proposed. However, the

calculated phase diagram of Al-Zn was not in good accord with her assessment on the basis of experimental data available in the literature. Mey and Effenberg [86Mey] subsequently re-evaluated this system thermodynamically and their calculated invariant temperatures for the eutectic equilibrium, the critical point, and the monotectoid equilibrium differ by 2.9, 13.3 and 5.0°C respectively from the assessed values. Moreover, the calculated phase boundaries of $fcc_2/(fcc_2+hcp)$, as well as those for the miscibility gap of the fcc phase, differ significantly from the experimental values.

It is noteworthy to point out Murray [90Mur] proposed a new thermodynamic description for Al-Zn system by introducing a new lattice stability of fcc-Zn. By using the newly optimized lattice stability, she was able to minimize the discrepancies between the calculated and experimental phase boundary values.

Therefore, the objective of the present study is to provide a new thermodynamic description for the Al-Zn system using the lattice stabilities accepted by the SGTE group [91Din]. The new description allows us to calculate phase diagram in better agreement with the experimental data.

2. Thermodynamic Models

2.1 The Pure Elements

The Gibbs energies of the pure component elements Al and Zn are represented by the following two-term equation
$$G = A - B T \tag{1}$$
where G is the Gibbs energy, T is the absolute temperature, and A and B are parameters whose values need to be determined from experimental data.

2.2 The Solution Phases (liquid, fcc and hcp)

The Redlich-Kister representation [48Red] is employed to describe the excess Gibbs energies of the three solution phases (liquid, fcc and hcp) in the Al-Zn system. Accordingly, the Gibbs energy for any of the solution phases is

$$G = x_{Al} \, {}^\circ G_{Al} + x_{Zn} \, {}^\circ G_{Zn} + RT \, (\, x_{Al} \ln x_{Al} + x_{Zn} \ln x_{Zn} \,)$$

$$+ \, x_{Al} x_{Zn} \sum_{i=0}^{m} L_i \, (\, x_{Al} - x_{Zn} \,)^i \tag{2}$$

where G is the Gibbs energy for any of the solution phases, ${}^\circ G_{Al}$, ${}^\circ G_{Zn}$ are the Gibbs energies of Al and Zn in their reference states, x_{Al}, x_{Zn} are the mole fractions of Al and Zn in the phase, and R is the gas constant. The temperature dependence of the parameter L_i has the same form as that of G given in Eq.(1), i.e.
$$L_i = A_i - B_i T \qquad (\, i = 0, ..., m \,) \tag{3}$$
Values of the parameters A_i and B_i need to be determined from the experimental data.

3. Data Analysis

Phase diagram and thermodynamic data for the Al-Zn system are used to optimize the parameter values of the thermodynamic models for the three phases. However, prior to carrying out the optimization, the available data are reviewed as given below.

3.1 Phase Diagram Data

As mentioned earlier, there exist three phases in the Al-Zn system, i.e., the liquid, fcc(Al) and hcp(Zn) phases [58Han, 83Mur]. The liquid, fcc and hcp phases form a eutectic reaction at 381°C with x_{Zn}^{L}=0.887, x_{Zn}^{fcc}=0.670 and x_{Zn}^{hcp}=0.972 [83Mur]. The thermodynamic behavior of the fcc phase deviates positively from an ideal solution, resulting in the formation of a miscibility gap at low temperatures with a critical temperature of 351.5°C at x_{Zn}^{fcc}=0.395 [58Han, 83Mur]. Below the critical temperature, there is a monotectoid reaction at 277°C which involves the two fcc phases, with $x_{Zn}^{fcc_1}$=0.165 and $x_{Zn}^{fcc_2}$=0.590, and the hcp phase with x_{Zn}^{hcp}=0.984 [83Mur].

Since 1897, many experiments have been carried out to determine the liquidus curve for the Al-Zn system [58Han, 65Ell, 69Shu, 83Mur]; most of which are in good agreement with each other [1897Hey, 24Isi, 24Tan, 38Gay, 43Pel, 45But, 49Pel, 49Sol]. For the (Al) solidus, many experimental data are available [22Han, 24Isi, 38Gay, 39Mor, 45But, 49Geb, 49Pel, 51Ell], but discrepancies exist in the composition region x_{Zn}=0.40~0.65. The assessment of Murray [83Mur] is accepted in the present study.

The fcc miscibility gap has also been studied by numerous groups of investigators [24Isi, 24Tan, 36Fin, 48Bor, 51Ell, 56Mue, 67Lar, 74Sim, 75Ter]. However, the experimental data are not in agreement with each other. Some earlier studies proposed a peritectic reaction at about 440°C [22Han, 24Isi, 24Tan], but this invariant reaction was denied in favor of a fcc miscibility gap at 351.5°C [36Fin, 38Gay] with x_{Zn}^{fcc}=0.395 [58Han, 83Mur].

The solid solubility data of both Al in Zn [23Pie, 24Tan, 36Aue, 36Bur, 36Ful, 40Loe, 50Hof, 52Pas] and Zn in Al [24Isi, 24Tan, 36Fin, 48Bor, 51Ell, 74Sim] are in good agreement with each other except for that of Zn in Al in the composition range x_{Zn}=0.10~0.165.

3.2 Thermodynamic Data

The lattice stabilities of the pure elements Al and Zn are listed in Table 1, which are accepted by the SGTE group [91Din].

For the liquid phase, the enthalpies of mixing at 953 K were determined by [63Wit] calorimetrically. The activities of Al were determined by Batalin and Beloborodova [68Bat], and Predel and Schallner [69Pre] using EMF methods, while those of Zn by Lutz and Voigt [63Lut], Bolsaitis and Sullivan [69Bol], and Yazawa and Lee [70Yaz] were determined using vapor pressure methods. Using phase equilibrium data and enthalpy data by means of

TABLE 1

Lattice Stabilities for Al and Zn [91Din]

Al	Zn
$^\circ G^L - ^\circ G^{fcc} = 10711.0 - 11.4744T$	$^\circ G^L - ^\circ G^{hcp} = 7322.0 - 10.5706T$
$^\circ G^{hcp} - ^\circ G^{fcc} = 5481.0 - 1.8000T$	$^\circ G^{fcc} - ^\circ G^{hcp} = 2969.8 - 1.5699T$

TABLE 2

Parameters for the Liquid, fcc and hcp Phases

Phase	Term	A (J/mol)	B (J/mol·K)	Reference States	
				Al	Zn
Liquid	L_0	10288	3.035	Liquid	Liquid
	L_1	-810	-0.471		
fcc	L_0	6656	-1.615	fcc	fcc
	L_1	6793	4.982		
	L_2	-5352	-7.261		
hcp	L_0	14620		hcp	hcp

TABLE 3

Comparisons Between the Assessed and Calculated Invariant Equilibria

Reaction		T(K)	Compositions (x_{Zn})	Reference
L = fcc + hcp	assessed	654.0	0.887-0.670-0.972	[83Mur]
	calculated	656.9	0.872-0.742-0.948	[86Mey]
	calculated	654.8	0.888-0.667-0.975	this study
$fcc_2 = fcc_1 + hcp$	assessed	550.0	0.590-0.165-0.984	[83Mur]
	calculated	555.0	0.604-0.166-0.965	[86Mey]
	calculated	550.7	0.592-0.145-0.985	this study
$fcc = fcc_1 + fcc_2$	assessed	624.5	0.395	[83Mur]
	calculated	611.2	0.362	[86Mey]
	calculated	622.3	0.344	this study

quantitative thermal analysis, Velisek [75Vel] calculated the activities of Al.

The activities of Al in solid alloys were measured by Hilliard *et al.* [54Hil], Corsepius and Muenster [59Cor], Ptak and Zabdyr [71Pta], and Miller *et al.* [72Mil] using EMF methods, while those of Zn were determined by measuring the partial pressures of Zn using a multiple rotating Knudsen source coupled with a mass spectrometer by Piacente *et al.* [76Pia], and using an atomic absorption by Takahashi and Asano [82Tak].

4. Optimization and Calculation

Values of the model parameters for the liquid, fcc and hcp phases are optimized using the experimental thermodynamic and phase equilibrium data available. The optimization is carried out using a PC-based program, BINOPT, developed by Chen, Zuo, Kao and Chang [93Che]. The basic strategy used in the program is to obtain a set of model parameters for all the phases by minimizing the objective function $Y^{calc}-Y^{exptl}$. The quantity Y denotes either $\overline{G}_i^j$, H^j, x_i^j and T with the subscript i being one of the component element and the superscript j being one of the phases. For instance, $\overline{G}_i^j$ is the partial Gibbs energy of component i in the j-phase and x_i^j is the composition of the component i for the j-phase. The temperature T stands for a specified temperature of a heterogeneous equilibrium, such as a eutectic temperature. The superscript 'calc' and 'exptl' for Y indicate the values of Y are either model-calculated or experimentally determined values. During the course of optimization, different weighting factors are assigned to the data points according to the degree of their reliability on the basis of our assessment. Values of the optimized solution parameters are given in Table 2.

Once the solution parameters are obtained, the phase diagram of Al-Zn as well as the various thermodynamic properties are calculated using the Lukas program, BINARY [82Luk, 88Luk] and plotted using the graphic program by Kattner *et al.* [90Kat]. Figure 1 shows the calculated phase diagram with the experimental data taken from the literature [1897Hey, 22Han, 23Pie, 24Isi, 24Tan, 36Aue, 36Bur, 36Fin, 36Ful, 38Gay, 39Mor, 40Loe, 43Pel, 45But, 48Bor, 49Geb, 49Pel, 49Sol, 50Hof, 51Ell, 52Pas, 56Mue, 67Lar, 74Sim, 75Ter]. Figure 2 shows a comparison between the model-calculated values for the integral enthalpies of mixing for the liquid phase at 953K and the experimental data of Wittig and Keil [63Wit]. Figures 3 and 4 show the model-calculated values of $\overline{G}_{Al}$ and $\overline{G}_{Zn}$ for the liquid phase at 1000K and for the fcc phase at 653K respectively.

In addition to Figures 1-4, the stability diagrams in terms of T versus $\overline{G}_{Zn}$ and 1/T versus $logP_{Zn}$ are calculated from the model parameters for the various phases as shown in Figures 5 and 6a. These two diagrams together with Figure 1 completely define the temperature-composition-$logP_{Zn}$(or $\overline{G}_{Zn}$) relationship for the Al-Zn binary system. In calculating the values of $logP_{Zn}$, the vapor pressures of pure Zn, P^o_{Zn}, according to Hultgren *et al.* [73Hull], are used as given below:
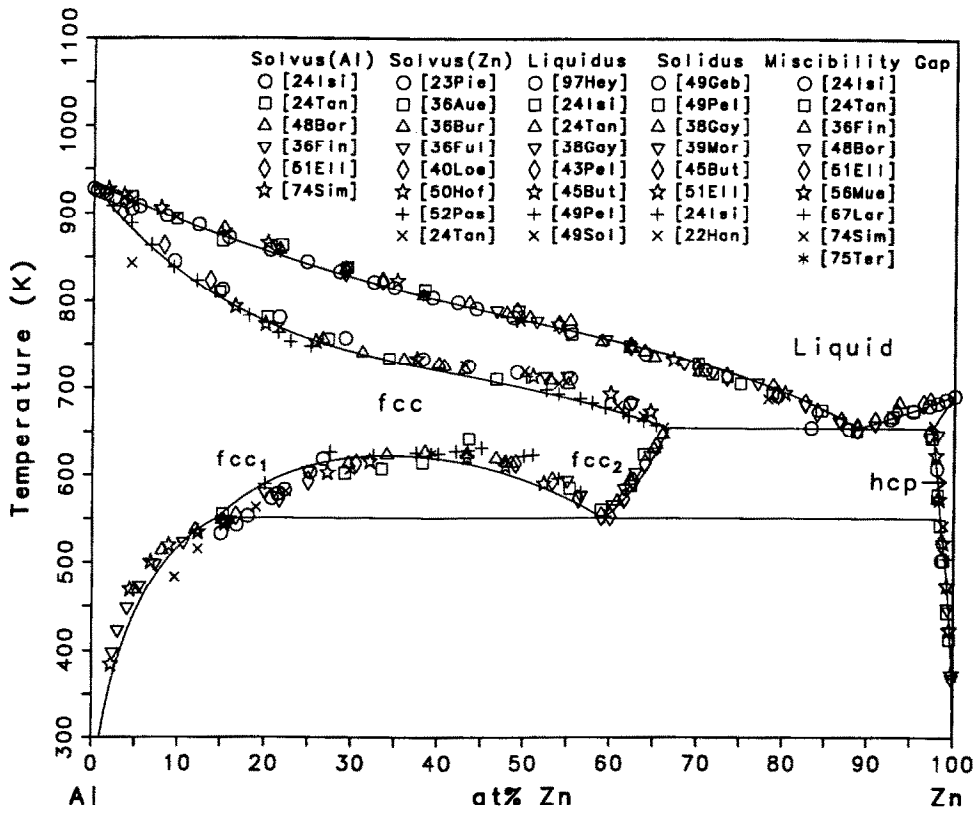
FIG. 1

Phase diagram of Al-Zn : comparison between the model-calculated diagram and experimental data
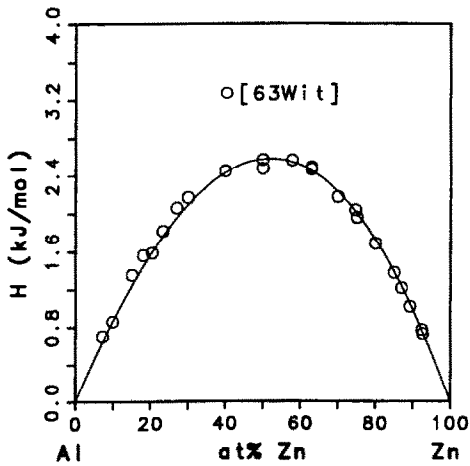

FIG. 2

The enthalpy of the liquid phase at 953 K, referred to Al(L) and Zn(L) : comparison between the model-calculated values and experimental data
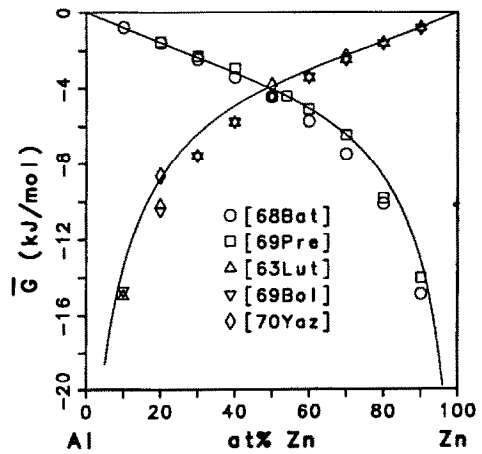

FIG. 3

The partial Gibbs energies of the liquid phase at 1000 K, referred to Al(L) and Zn(L) : comparison between the model-calculated values and experimental data
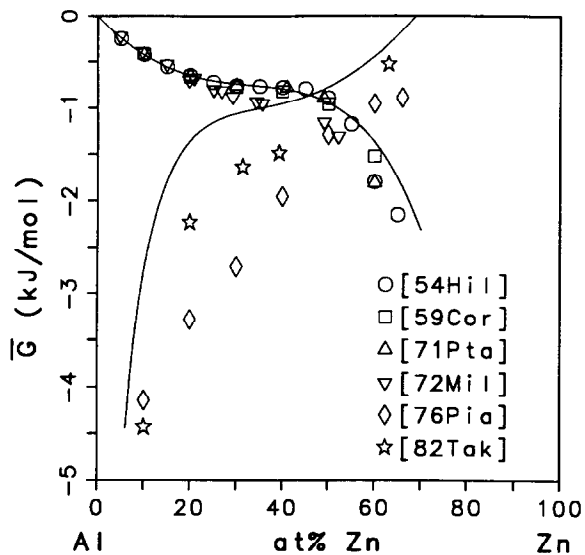
FIG. 4

The partial Gibbs energies of the fcc phase at 653 K, referred to Al(fcc) and Zn(hcp) : comparison between the model-calculated values and experimental data
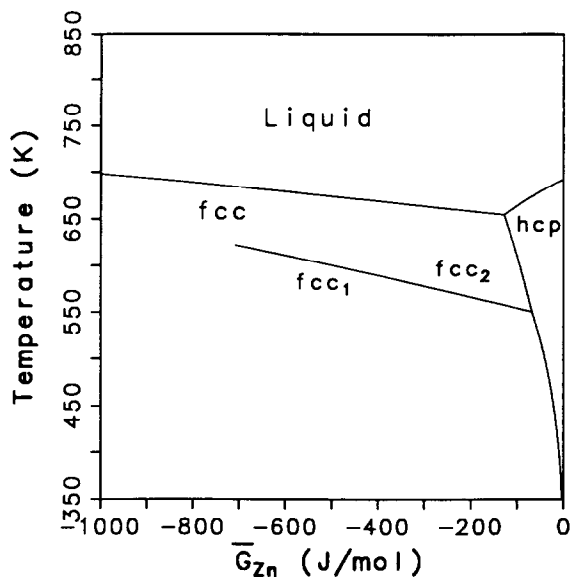

FIG. 5

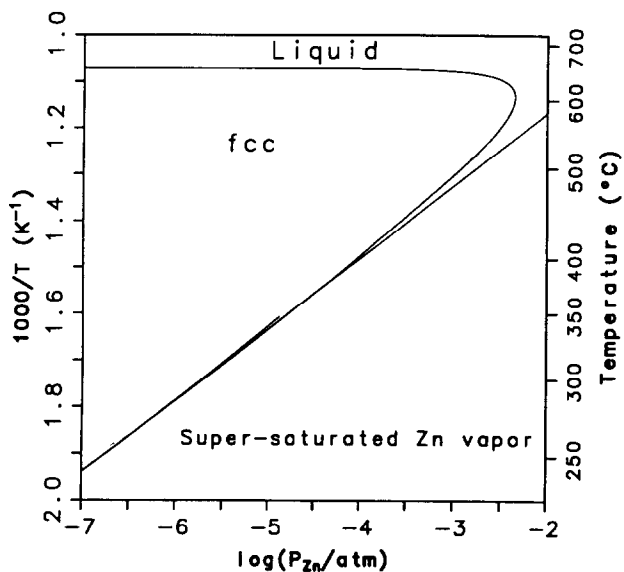Calculated stability diagram of Al-Zn in terms of T versus $\overline{G}_{Zn}$

FIG. 6a

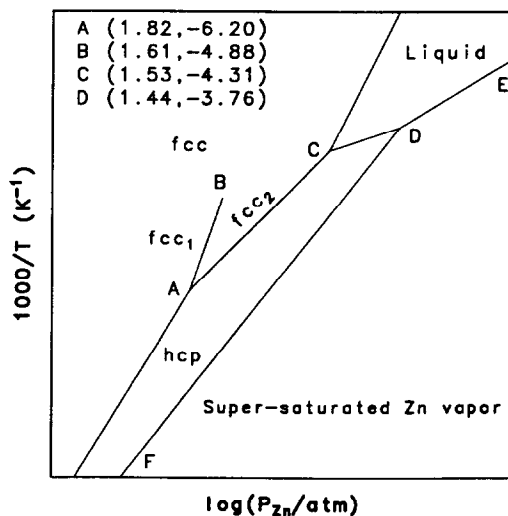Calculated stability diagram of Al-Zn in terms of 1000/T versus logP$_{Zn}$

FIG. 6b

An enlarged schematic diagram depicting the invariant equilibria of the Al-Zn system. Details of these equilibria cannot be resolved from the representation given in Fig. 6a

$$\log P^o_{Zn} \text{ (in atm)} = 10.108 - \frac{6904.9}{T} - 1.371 \log T \quad (298K \leq T \leq 692.7K) \tag{4}$$

$$\log P^o_{Zn} \text{ (in atm)} = 4.718 - \frac{6278.0}{T} + 0.208 \log T \quad (692.7K \leq T \leq 1180K) \tag{5}$$

Since details concerning the invariant equilibria cannot be resolved from the representation given in Figure 6a, an enlarged diagram depicting these equilibria is shown schematically in Figure 6b. Point A in this figure represents the monotectoid equilibrium, $fcc_2=fcc_1+hcp$. Point B is the critical point for the miscibility gap of the fcc phase. Point C is the eutectic equilibrium, $L=fcc_2+hcp$. Point D is essentially the triple point of the pure Zn, i.e., Zn(hcp), Zn(L) and Zn(g) co-exist under a total pressure of 1 atm. At any temperature higher than that corresponding to the triple point of Zn (i.e. point D), when $\log P_{Zn}$ is higher than that represented by line DE, pure Zn(L) may form. On the other hand, at any temperature lower than the triple point, when $\log P_{Zn}$ is higher than that represented by line DF, Zn(hcp) may form.

5. Discussion

As shown in Figure 2, there is excellent agreement between the model-calculated values for the integral enthalpies of mixing of the liquid alloys at 953K and the calorimetric data of Wittig and Keil [63Wit]. The model-calculated values of $\overline{G}^L_{Al}$ at 1000K are in excellent agreement with the EMF-measured values by Predel and Schallner [69Pre], as given in Figure 3. The calculated values are also in agreement with the data of Batalin and Beloborodova [68Bat] for values of $x_{Zn}<0.5$. At values of $x_{Zn}>0.5$, the calculated values are more positive by about 1 kJ/mol. On the other hand, the calculated values of $\overline{G}_{Zn}$ are more positive than the experimental data of Bolsaitis and Sullivan [69Bol] and Lutz and Voigt [63Lut] by vapor pressure measurement, but in agreement with that of Yazawa and Lee [70Yaz], which was also determined by vapor pressure method. Since values of $\overline{G}_{Zn}$ are related to those of $\overline{G}_{Al}$ by the Gibbs-Duhem relationship, the data of Bolsaitis and Sullivan [69Bol] and Lutz and Voigt [63Lut] are not consistent with the EMF data of Predel and Schallner [69Pre], and Batalin and Beloborodova [68Bat]. They are also inconsistent with the vapor pressure data of Yazawa and Lee [70Yaz].

As shown in Figure 4, the model-calculated values of $\overline{G}^{fcc}_{Al}$ for the fcc phase at 653K are also in agreement with the EMF-measured values of Hilliard et al. [54Hil], Corsepius and Muenster [59Cor] and Miller et al. [72Mil]. On the other hand, the values of $\overline{G}^{fcc}_{Zn}$ obtained from vapor pressure measurements by Piacente et al. [76Pia] and Takahashi and Asano [82Tak] are more negative than the calculated values. Since the calculated $\overline{G}^{fcc}_{Zn}$ values are consistent with the $\overline{G}^{fcc}_{Al}$ values by the Gibbs-Duhem relationship, the experimental data of the last two groups of investigators are not in accord with the data of Hilliard et al. [54Hil], Corsepius and Muenster [59Cor] and Miller et al. [72Mil], using EMF methods.

It is interesting to note that the model-calculated values for both the liquid and fcc

phases are in accord with the experimental data obtained by EMF methods, but not with that obtained by vapor pressure methods, except for the data of Yazawa and Lee [70Yaz].

Since the model-calculated values for the integral enthalpies and the partial Gibbs energies of Al for the liquid phase are in agreement with the calorimetric values (see Figure 2) and with the EMF-measured activities of Al (see Figure 3), there is a considerable degree of confidence in the reliability of the model parameters obtained for the liquid phase. Likewise, we believe the reliability of the parameters obtained for the fcc phase, since the model-calculated values of $\overline{G}_{Al}^{fcc}$ are also in agreement with the experimental values obtained by EMF methods.

We will next discuss the calculated phase diagram with the experimental data. As shown in Figure 1, good agreement is obtained between the calculated and experimental phase boundaries for the fcc+L, hcp+L and fcc+hcp two-phase fields. A comparison between the calculated and experimental values for the eutectic and monotectoid invariant equilibria is given in Table 3. The calculated temperatures are within 1°C from the assessed values; the calculated compositions are in agreement with the assessed values except for the composition of the fcc_1 phase at the monotectoid isotherm. This difference is only 2 at%.

The model description for the miscibility gap for the fcc phase is not in good accord with the experimental data. As shown in Figure 1, the model-calculated miscibility gap for the Zn-rich portion is too low in temperature while that for the Al-rich portion is too high in temperature. However, there are appreciable disagreements between the experimental data obtained by different groups of investigators for the miscibility gap and the fcc/(fcc+hcp) phase boundary. Since the model parameters are able to account for the thermodynamic data and the phase boundaries of fcc+L, hcp+L and fcc+hcp, we believe the model-calculated miscibility gap is a reasonable description of the actual situation.

Let us now re-examine the $\overline{G}_{Al}^{fcc}$ and $\overline{G}_{Zn}^{fcc}$ values at 653K given in Figure 4 in light of the fcc miscibility gap. The temperature of 653K is only about 30°C above the critical point. At this temperature, we would expect the Gibbs energy curve to be extremely flat from 25 to 45 at% Zn. This means the partial Gibbs energies would change slowly with composition as the calculated curves shown in Figure 4. Yet the values of $\overline{G}_{Zn}^{fcc}$ obtained by Piacente et al. [76Pia] and Takahashi and Asano [82Tak] change rapidly with composition. These phenomena indicate that something must be wrong with their data. Conversely, we would have to discard the phase diagram data as well as the $\overline{G}_{Al}^{fcc}$ values obtained by EMF methods.

The most thorough assessment and calculation of the Al-Zn binary to-date is that due to Mey and Effenberg [86Mey]. Their calculated temperatures and compositions of the invariant reactions are also given in Table 3 for comparison. For the eutectic reaction, their calculated temperature is 2.9°C higher than the assessed value based on experimental data; the compositions of x_{Zn}^{L}, x_{Zn}^{fcc} and x_{Zn}^{hcp} differ from the assessed values by -0.015, 0.072 and -0.024 respectively. For the monotectoid reaction, the calculated temperature and values of x_{Zn}^{fcc2}, x_{Zn}^{fcc1} and x_{Zn}^{hcp} differ from assessed values by 5°C, 0.014, 0.001 and -0.019 respectively. The calculated critical temperature for the miscibility gap of the fcc phase is 13.3°C too low.

Since Mey and Effenberg [86Mey] and we use the same total number of solution parameters to describe the thermodynamic properties of the liquid, fcc and hcp phases of Al-Zn, our description of this binary is an improvement over that of Mey and Effenberg [86Mey]. In other words, not only our model-calculated values of the thermodynamic properties are in accord with the experimental data, our calculated phase boundaries including the invariant equilibria are also in much better agreement with the experimental data than those calculated from the thermodynamic description of Mey and Effenberg [86Mey].

6. Conclusions

Using thermodynamic and phase equilibrium data available in the literature, a set of solution model parameters for the liquid, fcc and hcp phases were obtained by optimization. Thermodynamic values calculated from the models for the liquid and fcc phases are in agreement with the experimental values. The partial Gibbs energy values of Zn obtained by vapor pressure methods differ from the model-calculated values and experimental values obtained using EMF methods for both the liquid and fcc phases. These experimental values are believed to be in error. The discrepancies between the calculated and measured values by vapor pressure methods were also reported by previous calculations. The calculated phase equilibria including the invariant points are in much better agreement with the experimental values than previous calculations.

7. Acknowledgments

8. References

[1897Hey] C. T. Heycock and F. H. Neville, *J. Chem. Soc.*, **71** (1897) 389.

[22Han] D. Hanson and M. L. V. Gayler, *J. Inst. Met.* **27** (1922) 267-294.

[23Pie] W. M. Pierce and M. S. Palmerton, *Trans. AIME*, **68** (1923) 767.

[24Isi] T. Isihara, *Sci. Rep. Tohoku Univ.*, **13** (1924) 18-21.

[24Tan] T. Tanabe, *J. Inst. Met.*, **32** (1924) 415-427.

[36Aue] H. Auer and K. E. Mann, *Z. Metallkd.*, **28** (1936) 323-326.

[36Bur] A. Burkhardt, *Z. Metallkd.*, **28** (1936) 299-308.

[36Fin] W. L. Fink, *Trans. AIME*, **12** (1936) 244-260.

[36Ful] M. L. Fuller and R. L. Wilcox, *Trans. AIME*, **122** (1936) 231-246.

[38Gay] M. L. V. Gayler, M. Haughton and E. G. Sutherland, *J. Inst. Met.*, **63** (1938) 123-147.

[39Mor] T. Morinaga, *Nippon Kinzoku Gakkaishi*, **3** (1939) 216-221.

[40Loe] K. Loehberg, *Z. Metallkd.*, **32** (1940) 86-90.

[43Pel] E. Pelzel and H. Schneider, *Z. Metallkd.*, **35** (1943) 124-127.

[45But] E. Butchers and W. Hume-Rothery, *J. Inst. Met.*, **71** (1945) 291-311.

[48Bor] G. Borelius and L. E. Larsson, *Ark. Mat. Astr. Fys.*, **35A** (13) (1948) 1-14.

[48Red] O. Redlich and A. T. Kister, *Ind. Eng. Chem.*, **40** (1948) 345-348.

[49Geb] E. Gebhardt, *Z. Metallkd.*, **40** (1949) 136-140.

[49Pel] E. Pelzel, *Z. Metallkd.*, **40** (1949) 134-136.

[49Sol] I. S. Solet and H. W. St. Clair, Bureau of Mines Report of Investigations 4553 (1949).

[50Hof] W. Hofmann and G. Fahrenhorst, *Z. Metallkd.*, **42** (1950) 460-463.

[51Ell] E. C. Ellwood, *J. Inst. Met.*, **80** (1951) 217-224.

[52Pas] A. Pasternak, *Bull. Intern. Acad. Polon. Sci. Ser. A*, (1952) 177-192.

[54Hil] J. E. Hilliard, B. L. Averbach and M. Cohen, *Acta Metall.*, **2** (1954) 621-631.

[56Mue] A. Muenster and K. Sagel, *Z. Phys. Chem.*, **7** (1956) 296-316.

[58Han] M. Hansen and K. Anderko, *Constitution of Binary Alloys*, McGraw-Hill, New York, (1958).

[59Cor] H. Corsepius and A. Muenster, *Z. Phys. Chem.*, **22** (1959) 1-19.

[63Lut] G. J. Lutz and A. F. Voigt, *J. Phys. Chem.*, **67**(12) (1963) 2795-2799.

[63Wit] F. E. Wittig and G. Keil, *Z. Metallkd.*, **54**(10) (1963) 576-590.

[65Ell] R. P. Elliott, *Constitution of Binary Alloys*, First Supplement, McGraw-Hill, New York, (1965).

[67Lar] L. E. Larsson, *Acta Metall.*, **15** (1967) 35-44.

[68Bat] G. I. Batalin and E. A. Beloborodova, *Russ. Metallurgy*, **4** (1968) 121-125.

[69Bol] P. Bolsaitis and P. M. Sullivan, *Trans. AIME*, **245** (1969) 1435-1438.

[69Pre] B. Predel and U. Schallner, *Z. Metallkd.*, **60**(11) (1969) 869-877.

[69Shu] F. A. Shunk, *Constitution of Binary Alloys*, Second Supplement, McGraw-Hill, New York, (1969).

[70Yaz] A. Yazawa and Y. K. Lee, *Trans, Jap. Inst. Metals*, **11** (1970) 411-418.

[71Pta] W. Ptak and L. Zabdyr, *Arch. Hutn.*, **16** (1971) 253-267.

[72Mil] R. E. Miller, J. L. Straalsund and D. B. Masson, *Metall Trans.*, **3** (1972) 545-550.

[73Hul1] R. Hultgren, P. D. Desai, D. T. Hawkins, M. Gleiser, K. K. Kelley and D. D. Wagman, *Selected Values of the Thermodynamic Properties of the Elements*, American Society for Metals, Metals Park, Ohio, (1973).

[73Hul2] R. Hultgren, P. D. Desai, D. T. Hawkins, M. Gleiser, K. K. Kelley and D. D. Wagman, *Selected Values of the Thermodynamic Properties of Binary Alloys*, American Society for Metals, Metals Park, Ohio, (1973).

[74Sim] M. Simerska and P. Bartuska, *Czech. J. Phys.*, **B24** (1974) 553-559.

[75Ter] H. Terauchi, N. Sakamoto, K. Osamura and Y. Murakami, *Trans. Jpn. Inst. Met.*, **16** (1975) 379-383.

[75Vel] J. Velisek, *Kovove Mater.*, **13**(3) (1975) 303-313.

[76Pia] V. Piacente, V. Di Paolo and G. d'Ascenzo, *Thermochim. Acta*, **16** (1976) 63-68.

[82Luk] H. L. Lukas, J. Weiss, and E.-Th. Henig, *CALPHAD*, **6**(3) (1982) 229.

[82Tak] J. T. Takahashi and N. Asano, *Niihama Kogyo Koto Senmon Gakko Kiyo, Rikogakn Hen.*, **18** (1982) 78-84.

[83Mur] J. L. Murray, *Bull. Alloy Phase Diagrams*, **4**(1) (1983) 55-73.

[86Mey] S. an Mey and G. Effenberg, *Z. Metallkde*, **77**(7) (1986) 449-453.

[88Luk] H. L. Lukas, J. Weiss, U. Kattner, and E.-Th. Heig, *Manual of the Computer Programs, BINGSS, TERGSS, QUAGSS, BINFKT, TERFKT, QUAFKT AND PMLFKT*, Max Planck Institut für Metallforschung, Stuttgart, Germany, Version 11, (1988).

[89Che] S.-W. Chen, C.-H. Jan, J.-C. Lin and Y. A. Chang, *Metall. Trans.*, 20A, (1989) 2247-2258.

[90Kat] U. Kattner, National Institute of Standards and Technology, Gaithersburg, MD, private communication, 1990.

[90Mur] J. L. Murray, Alcoa Laboratories, Alcoa Center, PA, private communication, 1990.

[91Che] S.-W. Chen, Y.-Y. Chuang, Y. A. Chang and M. G. Chu, *Metall. Trans.*, 22A, (1991) 2837-2848.

[91Din] A. T. Dinsdale, *CALPHAD*, **15** (1991) 317-425.

[92Zuo] Y. Zuo and Y. A. Chang, (1992), unpublished results.

[93Che] S.-L. Chen, Y. Zuo, C. R. Kao and Y. A. Chang, *CALPHAD*, **17** (1993) 47-56.